The Genetic Signature of Perineuronal Oligodendrocytes

Sara Szuchet[1], Joseph A. Nielsen[2], Gabor Lovas[3], Javier Martinez de Velasco[2], Dragan Maric[4], Lynn D. Hudson[2]

Oligodendrocytes in the central nervous system can be categorized as precursors, myelin-forming, and non-myelinating perineuronal cells. The function of perineuronal oligodendrocytes is unknown; it was proposed that following injury, they may remyelinate denuded axons. We investigated these cells' potential. A combination of cell-specific tags, microarray technology and bioinformatics tools to identify gene expression differences between these subpopulations allowed us to capture the genetic signature of perineuronal oligodendrocytes. Here we report that perineuronal oligodendrocytes are configured for a dual role. As cells that embrace neuronal somata, they integrate a repertoire of transcripts designed to create their own code for communicating with neurons. But they maintain a reservoir of untranslated transcripts encoding the major myelin proteins for – we speculate – a demyelinating episode. We posit that the signature molecules, PDGFR-αβ, cytokine PDGF-CC, and transcription factor Pea3, used – among others - to define the non-myelinating phenotype, may be critical for mounting a myelinating programme during demyelination. Harnessing this capability is of therapeutic value for diseases such as multiple sclerosis. This is the first molecular characterization of an elusive neural cell.

[1]Department of Neurology, The University of Chicago, Chicago, IL, [2]Section of Developmental Genetics, National Institute of Neurological Disorders and Stroke, National Institutes of Health, Bethesda, MD, [3]Department of Neurology, Semmelweis University, Budapest, Hungary,

[4]Laboratory of Neurophysiology, National Institute of Neurological Disorders and Stroke, National Institutes of Health, Bethesda, MD.

Oligodendrocytes (OLGs) are morphologically and phenotypically diverse cells found in the central nervous system (CNS). This diversity was captured by del Rio Hortega, who in his 1928 monograph[1] described four subtypes of myelinating OLGs plus a separate class of non-myelinating OLGs that either appose neuronal somata (perineuronal) or extend their processes to envelop blood vessels (perivascular). Conceivably, each of these morphological entities is endowed with a unique function. Yet, OLGs are commonly defined as myelin producing cells with only an occasional reference to a non-myelinating OLG[2,3]. A detailed examination of the origins of OLG precursors (OLP) uncovered their complexity. Not only do spinal cord and hindbrain OLP originate from several dorsoventral domains that are differentially regulated by genes such as, e.g., *nkx6.1, olig2* and sonic hedgehog (Shh) signalling[4,5], but in the forebrain too, the generation of OLP is complex and dynamic[6,7]. Even the cerebral cortex may derive OLPs from more than one source, including an endogenous one[8,9]. These data stand as strong evidence for the diverse developmental origins of OLPs. And yet, no functional correlate to each of these subpopulations has been identified despite the fact that each of them has arisen from a distinct genetic program. Rather, the current view is that they are functionally equivalent and are competing for the same terrain[10,11]. From a simple teleological perspective, one could expect each class of precursor to become a distinct type of OLG within either the myelinating or non-myelinating families. The observation that after inducing the demise of one OLP population, another takes its place[10,11] may merely reflect the plasticity of these cells; i.e., we may conjecture that every OLG, independent of its assigned developmental function, might under circumstances of stress become a myelinating OLG.

To investigate the concept that a non-myelinating OLG has the capacity to transform into a myelinating cell, we examined its gene expression profile. We chose perineuronal OLGs (pN-OLGs) as representatives of non-myelinating cells because they are not normally connected to myelin but may have the potential to remyelinate denuded axons[12]. We had access to a polyclonal antibody (OTMP) that recognizes these cells. What is known about perineuronal OLGs? The morphology and ultrastructure of pN-OLGs are well defined. The interaction of pN-OLGs with neuronal somata is varied and complex[13,14]. In the simplest case of a one to one association, the pN-OLG indents a neuronal soma and embraces it with its processes. The issue of function remains a *tabula rasa*. It is generally assumed that pN-OLGs express myelin genes and proteins, but experimental evidence is still lacking. Nevertheless, if Ludwin's[12] report were to be confirmed, it would indicate that pN–OLGs possess a latent myelinating machinery that can be activated in a regenerating environment but is blocked during development. This is reminiscent of satellite Schwann cells that can remyelinate but are normally suppressed from ensheathing a "virgin" axon[15].

If, indeed, pN-OLGs constitute a reserve pool ready to undertake repair, enhancing their performance could be of help in demyelinating conditions. Harnessing this potential could have therapeutic applications for diseases such as multiple sclerosis. But to achieve this, we must have a good understanding of the genes and proteins expressed by pN-OLGs. We have undertaken to fill this void by examining the gene expression profile of these cells – marked by antibodies (Abs) $A_2B_5^+$/$OTMP^+$ - and defining their characteristics relative to the $A_2B_5^+$ progenitor and a dedicated O_4^+ OLG. Herein we provide compelling evidence that pN-OLGs are of an OLG lineage, e.g., they transcribe genes of all the major myelin proteins but do not translate them. Moreover, these and other data support the notion that pN-OLGs and O_4^+ cells

are progeny of $A_2B_5^+$ precursors. Despite this close lineal relationship, pN-OLGs have orchestrated a genetic program that sets them apart from both $A_2B_5^+$ precursors and O_4^+ OLGs. Notably, we observed a high level expression of the transcription regulator, Pea3, not previously recognized as a player within the OLG lineage. Ordinarily, pN-OLGs communicate with neuronal somata by a mechanism that remains to be elucidated. However, these cells harbour the capability of mounting a myelinating program should circumstances require it. To the best of our knowledge, this is the first molecular characterization of pN-OLGs. This research should open up new avenues for examining the function of these cells in health and disease.

The polyclonal antibody OTMP highlights perineuronal oligodendrocytes

In vitro, the immuno-purified polyclonal OTMP Ab co-localizes with mAb A_2B_5 on the surface of cultured live rat OLG progenitors but does not stain mature OLGs (Fig. S1). On rat brain tissue, this Ab singles out pN-OLGs in their varied morphological manifestations (Fig. 1A-C). This is not only the case for murine but also for human cells (Fig. 1D) and, presumably, other species (not tested). The Ab does not recognize neurons (Fig. 1 A-D), astrocytes (Fig.1E-G) or differentiated OLGs (Fig. 2D-F). We detected no co-localization with the Ab Iba1 on cortical microglial cells (not shown). Because both astrocytes and microglial cells may abut neuronal soma (arrowhead in Fig. 1D), although less frequently than OLGs[13,14], the selective identification of pN-OLGs by the OTMP Ab makes it an invaluable tool for not only unambiguously distinguishing these cells but, more importantly, for actually defining their phenotype.

$OTMP^+$ perineuronal cells are of OLG lineage but do not synthesize the major myelin/OLG proteins

It is generally assumed, but never proven, that pN-OLGs express myelin proteins. We tested this assumption by *in situ* double labelling these cells with OTMP and Abs that mark progenitors

and mature OLGs. To investigate the lineage of pN-OLGs, we labelled the cortex of a 7-day-old CNP/EGFP transgenic mouse with anti-GFP/OTMP. Because EGFP is driven by the CNP promoter (an OLG protein), the co-localization of the Abs (Fig. 2A-C) identified pN-OLGs as originating from OLP. This was substantiated by the finding of transcripts for all the major myelin proteins in these cells (Table 1). We then asked: are these transcripts translated? Myelin basic protein (MBP) is the most widely used and best characterized of the OLG/myelin proteins. MBP was not detected immunohistochemically in pN-OLGs at P14 (Fig. 2D-F) - a time point when myelinating OLGs have accumulated vast amounts of this protein. This was also the case for other OLG/myelin proteins such as $2^{'}$, $3^{'}$-cyclic nucleotide $3^{'}$ phosphodiesterase (CNPase), CC1/AP7/APC, proteolipid protein, and myelin associated glycoprotein (not illustrated). Collectively, these outcomes portray pN-OLGs to be of a non-myelinating phenotype but with the ability for mounting a myelinating program. This observation has broad implications, for if we could exploit this capability by interfering with the molecular cues that stop pN-OLGs from synthesizing myelin proteins, the cells could then activate an endogenous remyelination programme - an issue of importance for demyelinating diseases such as multiple sclerosis.

$A_2B_5^+$/OTMP$^+$cells are scattered throughout the developing brain

To monitor the developmental stages of non-myelinating cells, we co-labelled acutely isolated P7 and P14 rat brain cells with Abs OTMP and A_2B_5. The rationale for a dual label strategy stems from the *in vitro* evidence that a subpopulation of progenitors has both epitopes (Fig. S1). Fluorescence-activated cell sorting (FACS) of this subpopulation revealed heterogeneity in the intensity of staining within both the single labelled as well as the double labelled cells (Fig. 3). Indeed, the $A_2B_5^+$/OTMP$^+$ population can be subdivided into three distinct subgroups that differ in the relative intensity of the two markers. Quantitatively, there were no

appreciable changes in the dispersion of these groups between P7 and P14. This suggests that differences in the stage of development are not responsible for the observed heterogeneity. However, because the cells were derived from whole brain preparations, variation in regional compartments could account for cell diversity.

To assess this possibility, we dissected the CNS tissue into spinal cord, brain stem, basal ganglia, corpus callosum, and cortex at P0, P7 and P14 and repeated the experiments outlined above. Heterogeneity was still seen in every compartment examined (Fig. S2A-C), but there were interesting temporal and spatial differences in the distribution of the $A_2B_5^+/OTMP^+$ cells. Temporally, there was a significant increase in the number of these cells from a scattered few at P0 to a maximum at P7, when they averaged 12% of the total population. This may represent their steady state value as there was only a slight change by P14. The single labelled cells, $A_2B_5^+$ or $OTMP^+$**,** accounted for 16-22% of cells with only a small variation from P0 to P14. Regional differences were minimal in the $A_2B_5^+/OTMP^+$ group throughout the brain, but there was a slight increase in the brain stem, and a markedly low presence in the spinal cord (Fig. S2A-C). The single labelled cells exhibited no preferred localization within the brain or spinal cord. Collectively, these data show the $A_2B_5^+/OTMP^+$ cells to be located throughout the brain. It remains to be shown whether $A_2B_5^+/OTMP^+$ is a signature underlying a broad class of OLG lineage cells with the common denominator being that of belonging to the non-myelinating type or does it represent solely the pN-OLG?

The $A_2B_5^+/OTMP^+$ cell depicts a unique oligodendrocyte lineage phenotype

There is reliable experimental evidence that OLP originate from various sites and migrate throughout the CNS[4-7]. However, it has not been proven that they are grouped into subpopulations with distinct phenotypes. Functionally, there are at least three OLG subgroups:

precursor, myelinating and non-myelinating. Our discovery that we can place an immunological tag on non-myelinating cells opened up an opportunity to compare the molecular features of each of these OLG subpopulations. We used the Affymetrix microarray technology to identify gene expression patterns for cells recognized by the molecular markers $A_2B_5^+$, $A_2B_5^+/OTMP^+$, O_4^+ and $OTMP^+$. We chose the P7 stage of development because it still contains progenitors while myelination has also begun. Hence, P7 rat brain dissociates were labelled with each of these four markers and were individually purified by preparative FACS. mRNA was isolated from each of the purified fractions and processed as described in Methods Summary and Supplementary Information

We used the Principal Component Analysis on gene expression data to visualize the relationship between these groups (Fig. 4A). This analysis disclosed a sharp demarcation among the four populations. Notably, the OTMP Ab identified a subpopulation of $A_2B_5^+$ precursors with a distinct phenotype (Fig.4A). The transition from an $A_2B_5^+$ precursor to an O_4^+ committed OLG was analyzed by Nielsen *et al.*[16], who showed that the O_4^+ cell completely reorganizes its metabolism to assemble myelin. The $OTMP^+$ cell is not considered here. Our interest is on the $A_2B_5^+/OTMP^+$. To bring to light the genetic signature of the $A_2B_5^+/OTMP^+$ phenotype, we analyzed its expression profile relative to gene expression patterns of each, the $A_2B_5^+$ precursor and the O_4^+ committed cell, utilizing bioinformatics tools. Two general gene expression profiles describe the $A_2B_5^+/OTMP^+$ phenotype. In one, a cluster of genes exhibits higher levels of expression in the $A_2B_5^+/OTMP^+$ cell compared to both $A_2B_5^+$ and O_4^+ cells (Fig. 4B). The other displays a shallow positive slope between $A_2B_5^+$ and $A_2B_5^+/OTMP^+$ but a steep declining slope from $A_2B_5^+/OTMP^+$ to O_4^+ (Fig. 4C). Here we demonstrate that genes presumed to be crucial to the biology of the $A_2B_5^+/OTMP^+$ cell fall in either of these two categories.

$A_2B_5^+$/OTMP$^+$ cells express transcription factors judged essential for the generation of the OLG lineage in a context-dependent manner

There is a vast literature documenting the critical roles of the transcription factors (TFs) Dlx1/2, Olig1, Olig2, Sox10 and Mash1 in the acquisition of the myelinating fate. However, because of the diverse origins of OLP, and because the role of each of these TFs may vary in each region[17,18], we began by tracing the ancestry of the $A_2B_5^+$/OTMP$^+$ cell. Figure 4D (see also Fig. S3) shows that *dlx* transcripts are as high in the $A_2B_5^+$/OTMP$^+$ cell as in the A_2B_5 progenitor. Members of the *dlx* homeobox gene family serve as molecular markers for the progeny of embryonic basal forebrain multipotent stem cells capable of migrating long distances to populate the dorsal telencepalon and generating (*in vitro)* both GABAergic neurons and OLGs[19]. Indeed, *dlx1/2* genes have been shown to be essential for this migration[20]. Similarly, OLGs and astrocytes emigrating from the postnatal subventricular zone to inhabit white matter and the cerebral cortex have been reported to be descendants of a common *dlx*-expressing progenitor originating in the embryonic ventral telencephalon[7]. These reports and the finding of *dlx1* in $A_2B_5^+$/OTMP$^+$ cells (Fig. 4D) suggest that members of this population have a ventral forebrain ancestry.

We next proceeded to analyze the expression of these TFs in the $A_2B_5^+$/OTMP$^+$ cell. Interestingly, there is little quantitative difference in the TF transcripts between the A_2B_5 and $A_2B_5^+$/OTMP$^+$ cells but there is a pronounced variance relative to the O_4 cell (Fig. 4D).

Petryniak *et al.*[21] have recently elucidated the nature of the interactions among these TFs that ultimately dictate the fate of a cell to become a neuron or a myelinating OLG in the ventral telencephalon. For example, they report that Dlx1/2 negatively-regulate Olig2 whereas Mash1 restricts the number of Dlx1/2$^+$ cells, thus favouring OLGs over GABAergic neurons. The

involvement of Mash1 in conjunction with Olig2 in the specification of OLGs in the developing ventral forebrain was also reported by Parras *et al.*[22]. In light of these findings, it is instructive to examine the course followed by these TFs in $A_2B_5^+$/OTMP$^+$ relative to O_4^+ cells. The high level of *dlx1* transcript found in the $A_2B_5^+$/OTMP$^+$ cell (Fig. 4D) seems to fit its presumed role as an inhibitor of the myelinating phenotype [21]. However, the expression of *olig2* stays invariant in the three cell types (not shown). Similarly, the >5-fold higher level of *mash1* transcripts in $A_2B_5^+$/OTMP$^+$ cells does not agree with the Petryniak *et al.*[21] scheme. Another gene, s*ox9*, required for neuron-glial switch in the spinal cord[18], is >4-fold higher in the $A_2B_5^+$/OTMP$^+$ cell (not shown). Taken together, these results demonstrate that Dlx1, Olig2, Mash1 and Sox 9 behave in $A_2B_5^+$/OTMP$^+$ cells in a context-dependent manner that, presumably, eventuates in their acquisition of a non-myelinating fate. In contrast, Olig1 and Sox10, whose transcripts are upregulated ~3-fold and >30-fold, respectively, in O_4 cells (Fig. 4D) act according to their accepted role in determining the myelinating phenotype. Understanding <u>if</u> and <u>how</u> these transcription regulators specify the $A_2B_5^+$/OTMP$^+$ phenotype remains an exciting area for future research.

The transcription factor, Pea3, is a distinguishing feature of $A_2B_5^+$/OTMP$^+$ cells

The Pea3 group (Erm, Pea3 and Etv1) of Ets domain transcriptional regulators exhibits autoinhibitory activity that functions in a sumoylation-dependent fashion[23]. In specific motor neuron pools, Pea3 controls central position and terminal arborisation – a crucial step in the assembly of neuronal circuits[24]. It was shown that the glial cell-derived neurotrophic factor (GDNF) from target cells induces transcription of Pea3 in neurons[25]. Pea3 was also reported to be necessary for epidermal growth factor receptor (EGFR)-stimulated expression of metalloproteinases [26]. We observed a 52-fold increase in Pea3 transcripts in the non-myelinating

$A_2B_5^+$/OTMP$^+$ cell compared to the O_4^+ cell. This renders Pea3 as a beacon of the non-myelinating phenotype. Interestingly, Pea3 shares this status with another family member, Erm, which is expressed in peripheral satellite glia but not in myelinating Schwann cells [15]. The fact that members of the same family of TFs are used to demarcate the two phenotypes in both the CNS and PNS suggests that a common (or similar) mechanism underlies their segregation. Deciphering the function of these TFs is a goal for future research.

Signalling pathways that may be determinants in specifying the $A_2B_5^+$/OTMP$^+$ cell

To illuminate our understanding of the cellular processes that guide an A_2B_5 precursor towards either a non-myelinating ($A_2B_5^+$/OTMP$^+$) or a myelinating (O_4) phenotype, we started by comparing, in pairs (i.e., $A_2B_5^+$/OTMP$^+$/A_2B_5 or /O_4), the expression profiles of molecules known to play critical roles in patterning the CNS. Sonic hedgehog (Shh) and Wingless (Wnt) fall into this category. In addition to their cognate receptors, Patched and Smoothened (for Shh) and Frizzled (for Wnt), they require at least one essential co-receptor – LRP – a member of the low density lipoprotein receptor-related family and heparan sulfate proteoglycans (HSPGs) for transport and signal transduction. There is a large body of experimental evidence demonstrating the vital importance of these signalling molecules in specifying oligodendrogenesis[27-31,10], but the full range of their action has yet to be unravelled. However, the core molecular players have been identified. We used this knowledge to assess whether these morphogens have any part in specifying the $A_2B_5^+$/OTMP$^+$ cell. We found a >7- and >9-fold augmentation, respectively, of the Smoothened (*Smo*) and *Gli* transcripts in the $A_2B_5^+$/OTMP$^+$ cells compared to $A_2B_5^+$ and O_4^+ cells. Such a metabolic investment by this cell indicates that it has access to a source of Shh, and that there is a functional objective to be attained.

Shh is required for the expression of PDGFR-α[27], considered to be one of the earliest markers for OLPs. Significantly, at a time when PDGFR-α is no longer detected in the O_4^+ cell, we find a 7.2-fold upregulation of its transcripts in the $A_2B_5^+$/OTMP$^+$ cell. Data analysis suggests that Shh has a part in this event (Fig. S4). Of biological relevance is our observation that $A_2B_5^+$/OTMP$^+$ cells incorporate this receptor in a context-specific role. In addition to *pdgf-α,* the cells transcribe *pdgfR-β* and the cytokine *pdgf-c* – a high-affinity ligand for PDGFR-αβ and a strong mitogen[32]. The network in Fig.5A depicts predicted interactions among these and other molecules based on well-characterized systems. We posit that the binding of secreted PDGF-CC to the α- and β-PDGF receptor effects their association into the PDGFR-αβ heterodimer, thus silencing the response of $A_2B_5^+$/OTMP$^+$ cells to PDGF-AA - a ligand for the myelinating phenotype. Tacitly, this event specifies the $A_2B_5^+$/OTMP$^+$ fate. The usage of the cytokine PDGF-CC creates an autocrine loop that serves not only to control receptor activity but also cell numbers. Although the molecular mechanism underlying these interactions remains to be solved, the interactions per se can be viewed as a step toward establishing the $A_2B_5^+$/OTMP$^+$ phenotype.

Turning to Wnt, it is perhaps one of the most versatile morphogens, regulating as it does gene expression, cell fate, cell adhesion, and cell polarity. All the three vertebrate Wnt pathways use the frizzled (Fzd) receptor but the adaptor proteins vary[33,34]. The Wnt/β-catenin pathway directs the sequential onset of neurogenesis and gliogenesis[30] and prevents the differentiation of OLP[31]. To appreciate how critical Wnt signalling must be to the biology of $A_2B_5^+$/OTMP$^+$ cells, it suffices to note that the Fzd2 transcript is 14-fold higher in $A_2B_5^+$/OTMP$^+$ cells than in O_4^+ cells. To derive a cell-specific role for Wnt signalling, we analyzed the gene profile using interactive networks. Setting aside the well-known gene repertoire controlled by Wnt - all of which are highly expressed by the $A_2B_5^+$/OTMP$^+$ cells (Fig. 5B) - one protein, Nr-CAM, appears

as a likely downstream target of Wnt signalling because of the known LEF1 binding to Nr-CAM promoter[35]. Nr-CAM is a transmembrane adhesion molecule of the Ig superfamily. It is found in neurons and Schwann cells, but not in OLGs. Nr-CAM is critical in the early events of node of Ranvier formation in the PNS[36]. There is an 11-fold upregulation of the *nr-cam* transcript in $A_2B_5^+$/OTMP$^+$ cells. We postulate that Nr-CAM might serve as a point of contact with a neuron in a direct cell to cell contact as exemplified in Fig. 1A as well as through cellular processes as are seen in Fig. 1B. Other molecules may then modulate and strengthen these interactions.

As illustrated in Fig. 1, the pN-OLG either abuts a neuronal soma or contacts it through its processes. Hence, it was relevant to investigate signalling pathways that are transduced by direct cell to cell contact. The Notch and the Eph/ephrin pair act in this manner. In the fly, Notch inhibits differentiation by lateral signalling and controls cell fate by inductive interactions [37]. In vertebrates, it may additionally diversify progenitor populations [38]. The network shown in Fig. 5C brings to light three aspects of Notch signalling in $A_2B_5^+$/OTMP$^+$ cells. First, we noticed a transcriptional activation (>5-fold) of the bHLH TF ASCL1/Mash1 (Fig. 5C). During neurogenesis, there is a tight cross-regulation between Notch and the two TFs, Mash1 and Dlx1/2, that eventuates in sequential specification of progenitors[39]. Whether or how these factors specify the $A_2B_5^+$/OTMP$^+$ cell is still an open question. Nonetheless, our results support the idea that in $A_2B_5^+$/OTMP$^+$ cells, these two TFs together with Olig2 engage in a context-specific interplay that differs from their behaviour in, e.g., OLGs (Fig. 4D). Second, we observed the (>13-fold) upregulation of *hes5* (Fig. 5C), a Notch target and an inhibitor of myelin gene expression[40]. Finally, Fig. 5C implicates Notch1 in the elevated transcription in $A_2B_5^+$/OTMP$^+$ cells of lipocalin-prostaglandin D2 synthase (L-PGDS), also known as β-Trace. This is puzzling

for Notch1 has been shown to decrease PGDS expression, but the $A_2B_5^+$/OTMP$^+$ cells reveal elevated levels of both Notch1 and PGDS.

The Eph receptors and the ephrins are transmembrane tyrosine kinases. Their binding and subsequent clustering transduce bidirectional signals that regulate cell migration, adhesion or repulsion. This interaction requires direct cell to cell contact. A large number of other proteins modulate the outcome[41-43]. We have utilized an Eph/ephrin canonical pathway to assess the expression of these tyrosine kinase receptors in the $A_2B_5^+$/OTMP$^+$ cells. Significantly, we noted a selected transcription of the *ephA2,4,5* class of receptors and class *b3* ephrins in the $A_2B_5^+$/OTMP$^+$ pathway (Fig. 5D). Since their interaction is mostly between members of the same class, this allows the $A_2B_5^+$/OTMP$^+$ cells to be receivers of either forward or reverse signalling. That the latter may be of physiological significance for these cells can be surmised from both the expression of the G-coupled CXCR4 receptor and its ligand SDF-1 (Fig. 5D) and from evidence of their participation together with ephrin-B in controlling migration in other cell types (e.g., granule cells)[44,45]. One attractive feature of the Eph/ephrin signalling is that it fosters cell to cell attachment and detachment. The action is not strictly reversible as cell separation requires endocytosis or proteolysis. Nevertheless, it does provide flexibility for cells to engage or disengage when circumstances demand it. As argued below, we speculate that pN-OLGs may avail themselves of this prerogative in specific circumstances.

The $A_2B_5^+$/OTMP$^+$ cell amasses a complex extracellular matrix

The $A_2B_5^+$/OTMP$^+$ gene profile presented here is cell-specific (i.e., it contains only those transcripts that differ from A_2B_5 or O_4). Therefore, assessment of its contribution to the ECM may assist in identifying events that control the casting of the non-myelinating phenotype.

Examination of the $A_2B_5^+$/OTMP$^+$ transcripts revealed an unusual richness of adhesion molecules, receptors, and ECM molecules. Their levels of expression range from >3 to >7 compared to either $A_2B_5^+$ or O_4^+. It is reasonable to assume that such a metabolic investment signifies that the corresponding proteins are synthesized. To gain a glimpse of the context in which these proteins are utilized and their regulation, we examined them as part of interacting networks (Figs. 6A-D). Fig. 6A predicts the extracellular accumulation of collagens, including the unusual Col18A1 - a HSPG - nidogen, and reelin. In Fig.6B there is a display of members of the bone morphogenetic protein (BMP) family, their receptors, the inhibitor noggin and the receptor endoglin. There is an indication that the secretion of collagens and BMPs as well as activation of the BMPR1/2 may be controlled by members of the TGFβ/BMP receptor/ligand family because of the downregulation of the transcription regulator SMAD7 - an inhibitor of TGFβ/activin and BMP signalling[46]. It is the interplay and fine tuning of these molecules together with other morphogens that, ultimately, demarcate cell fate[39,47].

Fig. 6C exhibits a display of metalloproteases (MMPs), their inhibitors and the chondroitin sulfate proteoglycan (CSPG), versican, mostly orchestrated by the Erb-B2 tyrosine kinase, in part for its own usage as it needs MMPs for signalling[48]. But Fig. 6C also indicates an interface with other signalling pathways, e.g., Shh, as its co-receptor LRP1 appears to be interacting with several components. The complex cross-talk between the ECM and the cell can be further appreciated in Fig. 6D, where we see apolipoprotein E and α2-macroglobulin, both secreted by the $A_2B_5^+$/OTMP$^+$ cell, as having a direct impact on LRP1. Another highly expressed (> 7-fold) secretory product, spondin, modulates Wnt by inhibiting its co-receptor, LRP5/6[49].

Discussion

In this work we sought to obtain the genetic signature of pN-OLGs by tabulating only those genes that differed significantly (> 2-fold) from either the $A_2B_5^+$ OLP or the O_4^+ OLG. The outcome revealed an OLG lineage cell with a novel phenotype (Figs. 4B-D). By adopting the PDGFR-αβ and its high affinity ligand, PDGF-CC (Fig. 5A), the A2B5$^+$/OTMP$^+$ cell has effectively demarcated a boundary between itself and the other members of its lineage. But the most notorious feature of this phenotype is that it has amalgamated genes pertaining to Schwann cell lineages. To begin with, the usage of the Ets domain transcription regulator, Pea3, presumably to establish and/or control the phenotype per se, mimics satellite Schwann cells [15]. Likewise, the secretion of fibrous collagens, nidogen (Fig. 6A) and the high level expression of NrCAM (Fig. 5B), and $\alpha_7\beta_1$ integrin (not shown) by A2B5$^+$/OTMP$^+$ cells are atypical for OLG lineages but are part of the Schwann cell repertoire. Notwithstanding these similarities, pN-OLGs and satellite Schwann cells function in a distinctive fashion[50]. We interpret these results as indicating that pN-OLGs have developed a code for communicating with neurons that differs significantly from the one used by myelinating OLGs. This finding brings to the fore an intriguing possibility. It is well known that the interaction between a myelinating OLG and an axon varies from a one to one relationship - not unlike that of the Schwann cell - to one plus many axons[51]. Could different codes be used for each case? Deciphering the way in which the structure of the pN-OLG ECM and plasmalemma influence cell to cell interaction should illuminate the broader issue of OLG-neuron interaction.

Our finding that pN-OLGs belong to the OLG lineage raises the question of lineage progression. This is particularly so because the embryonic and early postnatal $A_2B_5^+$ cell is highly heterogeneous (Fig. 3) and generates a varied progeny[52,53]. The work here pertains to a P7 $A_2B_5^+$ cell acutely isolated from a whole brain dissociate. We have demonstrated that the $A_2B_5^+$

cell, long-accepted as an OLG progenitor and shown to be a necessary intermediate in the path towards a myelinating phenotype[54], can also take a different route and become an $A_2B_5^+$/$OTMP^+$ cell, i.e., non-myelinating (Fig. 4A). Given that an $A_2B_5^+$ cell is the founder of both phenotypes, the challenge remains to discover at what stage of development they emerge. Is lineage progression linear or branched? And, more importantly, who triggers the signal? Is it cell-autonomous or does it depend on an extracellular induction? In this context, our discovery that $A_2B_5^+$/$OTMP^+$ cells express high levels of the TF Pea3 together with the suggestion that Erm - a member of the Pea3 group - is involved in driving Schwann cell precursors toward a satellite phenotype[15] makes Pea3 a bona fide contender for a role in creating/maintaining the $A_2B_5^+$/$OTMP^+$ non-myelinating phenotype. The lineage progression from peripheral ganglia precursors to Schwann cells has been postulated to involve an Erm^+ cell intermediate[15]. Could this also be the case for OLGs? The data herein set the stage to search for the answer.

A long-standing issue has been defining the function of pN-OLGs. It has been reported that, after injury, pN-OLGs protect themselves and neurons from apoptosis by upregulating L-PGDS [55]. But here we have identified a physiological high level of L-PGDS (Inset Fig. 5C). The question is, to what end? L-PGDS has a restricted distribution and a dual function[56]. As an enzyme, it catalyzes the conversion of prostaglandin H2 to D2; but as a lipocalin, it is a transporter of hydrophobic molecules. In brain cell lines, L-PDGS is activated by protein kinase C through a mechanism of de-repression of Notch-Hes signalling [57]. While not denying that L-PGDS may be important to the physiology of the pN-OLGs, more research is required to define its impact on pN-OLG function. The work by Yamazaki *et al.*[58] showing a bidirectional interaction between perineuronal astrocytes and neurons in the CA1 region of the rat hippocampus raises the intriguing possibility that pN-OLGs may engage in a related activity.

Indeed, synaptic signalling between GABAergic interneurons and OLP has been reported by Lin and Bergles[59]. However, their description of the cell as having a round soma with no visible processes does not correspond to the morphology of pN-OLGs. Nonetheless, it is of interest that pN-OLGs express GABA receptors (Fig. 5B). Undoubtedly, this is a research venue worth pursuing.

It has been proposed that pN-OLGs can partake in remyelination[60]. Our results indicate that they have the molecular armamentarium to respond to a demyelinating eventuality. They retain the capacity for migration and proliferation; they have receptors, signalling and ECM molecules they would need but, most importantly, they carry transcripts for all the major myelin proteins (Table 1). Furthermore, there is a 32-fold upregulation of the EGFR in pN-OLGs *vs* O_4 OLGs. This is striking in view of the report by Aguirre *et al.*[61] that the EGFR regulates oligodendrogenesis and remyelination. While this receptor must be physiologically engaged in functions other than remyelination, its high presence, per se, is an assurance that it can play its part when called upon.

One could envision a scenario where, in response to a demyelinating insult, the cell would use the Eph/ephrin bonds to detach from the neuron. The cytokine PDGF-CC - sequestered in the ECM in its latent form – would be exposed to proteolytic enzymes (accompanying trauma), thereby liberating its growth factor domain for interaction with the PDGFR-αβ; proliferation would then ensue in an asymmetric fashion. One daughter cell would rejoin the neuron; the other would activate its myelinating program to repair the damage. The description herein of the genetic signature of pN-OLGs should open up vistas for testing these hypotheses and, thereby, advance our knowledge of the biology and function of these cells.

METHODS SUMMARY

Immunohistochemistry of rodent and human brain. Animals were handled according to NIH guidelines. C57BL/6 mice or Sprague Dawley rats (Taconic Farms, Germantown, NY) were anesthetized by intraperitoneal injection of Xylazine plus Ketamine and perfused through the heart with PBS followed by 4% paraformaldehyde in PBS. The brains were removed and sectioned with a vibratome into 15-20 μm sections. Staining was done on free-floating sections. Experimental details of staining and analysis can be found in Supplementary Information.

Human tissue. Primary motor cortex samples originated from individuals whose autopsies revealed no central nervous system disorder. The tissue was supplied by the Department of Forensic Medicine, Semmelweis University Medical School and handled in Budapest (Hungary), an activity reviewed by the Office of Human Subjects Research, NIH (OHSR #2481). Processing is described in Supplementary Information.

Cell preparation and sorting. Cell preparation and isolation was performed as previously described[16].

Fluorescence-Labeled Cell Sorting (FACS) of Rat Oligodendrocytes. Whole brains were dissected from P7 and P14 rats, and the cerebellum and meninges were removed. The brains were kept in 4˚C wash buffer (Hanks buffer pH 7.4, 20mM Hepes, 50μg/ml gentamicin, and 0.1% bovine serum albumin). Labeled cell suspensions were prepared with papain digestion and analyzed using a FACSTAR^{+} flow cytometer (Becton Dickinson, Mountain View, CA). Three independent experiments were performed on P7 animals and 2 independent experiments on P14 animals. Experimental details are given in Supplementary Information.

Microarray. Total RNA was extracted using the RNeasy micro kit (Qiagen. Valencia, CA). The quality of total RNA was assessed using Agilent's Bioanalyzer microchip (Palo Alto, CA). 100 ng of total RNA was amplified following Affymetrix's small sample labeling protocol (vII). The

protocol contains two rounds of reverse transcription and *in vitro* transcription with the biotin label being incorporated during the second round of *in vitro* transcription. The raw data will be deposited in the Gene Expression Omnibus accessible at http://www.ncbi.nlm.nih.gov/geo/ Pathway and network analyses were performed with KEGG [62] and Ingenuity (Redwood City, CA).

1. Del Rio Hortega, P. Tercera aportacion al conocimiento morfologico e interpretacion functional de la oligodendroglia. *Mem R Soc Esp Hist Nat* **14,** 5-122 (1928).
2. Zerlin, M., Milosevic, A. & Goldman, J. E. Glial progenitors of the neonatal subventricular zone differentiate asynchronously, leading to spatial dispersion of glial clones and to the persistence of immature glia in the adult mammalian CNS. *Dev Biol* **270**, 200-13 (2004).
3. Menn, B. et al. Origin of oligodendrocytes in the subventricular zone of the adult brain. *J Neurosci* **26**, 7907-18 (2006).
4. Vallstedt, A., Klos, J. M. & Ericson, J. Multiple dorsoventral origins of oligodendrocyte generation in the spinal cord and hindbrain. *Neuron* **45**, 55-67 (2005).
5. Cai, J. et al. Generation of oligodendrocyte precursor cells from mouse dorsal spinal cord independent of *Nkx6* regulation and *Shh* signaling. *Neuron* **45**, 41-53 (2005).
6. Kessaris, N. et al. Competing waves of oligodendrocytes in the forebrain and postnatal elimination of an embryonic lineage. *Nat Neurosci* **9**, 173-9 (2006).
7. Marshall, C. A. & Goldman, J. E. Subpallial dlx2-expressing cells give rise to astrocytes and oligodendrocytes in the cerebral cortex and white matter. *J Neurosci* **22**, 9821-30 (2002).
8. Birling, M. C. & Price, J. A study of the potential of the embryonic rat telencephalon to generate oligodendrocytes. *Dev Biol* **193**, 100-13 (1998).
9. Gorski, J. A. et al. Cortical excitatory neurons and glia, but not GABAergic neurons, are produced in the Emx1-expressing lineage. *J Neurosci* **22**, 6309-14 (2002).

10. Richardson, W. D., Kessaris, N. & Pringle, N. Oligodendrocyte wars. *Nat Rev Neurosci* **7**, 11-18 (2006).
11. Ventura, R. E. & Goldman, J. E. Telencephalic oligodendrocytes battle it out. *Nat Neurosci* **9,** 153-4 (2006).
12. Ludwin, S. K. The function of perineuronal satellite oligodendrocytes: an immunohistochemical study. *Neuropathology and Applied Neurobiology* **10**, 143-149 (1984).
13. Polak, M., Haymaker, W., Johnson, J. E., Jr & D'Amelio, F. in *Histology and Histopathology of the Nervous System* (eds. Haymaker, W. & Adams, R. D.) 363-480 (Charles C. Thomas, Publisher, Springfield, IL, 1982).
14. Raine, C. S. in *Textbook of Neuropathology* (eds. Davis, R. L. & Robertson, D. M.) 137-164 (Williams & Wilkins, Baltimore, 1997).
15. Hagedorn, L. et al. The Ets domain transcription factor Erm distinguishes rat satellite glia from Schwann cells and is regulated in satellite cells by neuregulin signaling. *Dev Biol* **219**, 44-58 (2000).
16. Nielsen, J. A., Maric, D., Lau, P., Barker, J. L. & Hudson, L. D. Identification of a novel oligodendrocyte cell adhesion protein using gene expression profiling. *J Neurosci* **26**, 9881-91 (2006).
17. Tekki-Kessaris, N. et al. Hedgehog-dependent oligodendrocyte lineage specification in the telencephalon. *Development* **128**, 2545-54 (2001).
18. Rowitch, D. H. Glial specification in the vertebrate neural tube. *Nat Rev Neurosci* **5**, 409-19 (2004).
19. He, W., Ingraham, C., Rising, L., Goderie, S. & Temple, S. Multipotent stem cells from the mouse basal forebrain contribute GABAergic neurons and oligodendrocytes to the cerebral cortex during embryogenesis. *J Neurosci* **21**, 8854-62 (2001).
20. Anderson, S. A., Eisenstat, D. D., Shi, L. & Rubenstein, J. L. Interneuron migration from basal forebrain to neocortex: dependence on Dlx genes. *Science* **278**, 474-6 (1997).
21. Petryniak, M. A., Potter, G. B., Rowitch, D. H. & Rubenstein, J. L. Dlx1 and Dlx2 control neuronal versus oligodendroglial cell fate acquisition in the developing forebrain. *Neuron* **55**, 417-33 (2007).

22. Parras, C. M. et al. The proneural gene *Mash 1* specifies an early population of telencephalic oligodendrocytes. *J Neurosci* **27**, 4233-4242 (2007).
23. Degerny, C., de Launoit, Y. & Baert, J.-L. ERM transcription factor contains an inhibitory domain which functions in sumoylation-dependent manner. *Biochim Biophys Acta* doi:10.1016/j.bbagrm.2008.01.002 (2008).
24. Livet, J. et al. ETS gene Pea3 controls the central position and terminal arborization of specific motor neuron pools. *Neuron* **35**, 877-92 (2002).
25. Haase, G. et al. GDNF acts through PEA3 to regulate cell body positioning and muscle innervation of specific motor neuron pools. *Neuron* **35**, 893-905 (2002).
26. Cowden Dahl, K. D., Zeineldin, R. & Hudson, L. D. PEA3 is necessary for optimal epidermal growth factor receptor -- stimulated matrix metalloproteinase expression and invasion of ovarian tumor cells. *Mol Cancer Res* **5**, 413-421 (2007).
27. Nery, S., Wichterie, H. & Fishell, G. Sonic hedgehog contributes to oligodendrocyte specification in the mamalian forebrain. *Development* **128**, 527-540 (2001).
28. Murray, K., Calaora, V., Rottkamp, C., Guicherit, O. & Dubois-Dalcq, M. Sonic hedgehog is a potent inducer of rat oligodendrocyte development from cortical precursors in vitro. *Mol Cell Neurosci* **19**, 320-32 (2002).
29. Agius, E. et al. Converse control of oligodendrocyte and astrocyte lineage development by Sonic hedgehog in the chick spinal cord. *Dev Biol* **270**, 308-21 (2004).
30. Kasai, M., Satoh, K. & Akiyama, T. Wnt signaling regulates the sequential onset of neurogenesis and gliogenesis via induction of BMPs. *Genes Cells* **10**, 777-83 (2005).
31. Shimizu, T. et al. Wnt signaling controls the timing of oligodendrocyte development in the spinal cord. *Dev Biol* **282**, 397-410 (2005).
32. Reigstad, L. J., Varhaug, J. E. & Lillehaug, J. R. Structural and functional specificities of PDGF-C and PDGF-D, the novel members of the platelet-derived growth factors family. *Febs J* **272**, 5723-41 (2005).
33. Schambony, A., Kunz, M. & Gradl, D. Cross-regulation of Wnt signaling and cell adhesion. *Differentiation* **72**, 307-18 (2004).
34. Cadigan, K. M. & Liu, Y. I. Wnt signaling: complexity at the surface. *J Cell Sci* **119**, 395-402 (2006).

35. Conacci-Sorrell, M. E. et al. Nr-CAM is a target gene of the beta-catenin/LEF-1 pathway in melanoma and colon cancer and its expression enhances motility and confers tumorigenesis. *Genes Dev* **16**, 2058-72 (2002).
36. Custer, A. W. et al. The role of the ankyrin-binding protein NrCAM in node of Ranvier formation. *J Neurosci* **23**, 10032-9 (2003).
37. Louvi, A. & Artavanis-Tsakonas, S. Notch signalling in vertebrate neural development. *Nat Rev Neurosci* **7**, 93-102 (2006).
38. Yoon, K. & Gaiano, N. Notch signaling in the mammalian central nervous system: insights from mouse mutants. *Nat Neurosci* **8**, 709-15 (2005).
39. Yung, S. Y. et al. Differential modulation of BMP signaling promotes the elaboration of cerebral cortical GABAergic neurons or oligodendrocytes from a common sonic hedgehog-responsive ventral forebrain progenitor species. *Proc Natl Acad Sci U S A* **99**, 16273-8 (2002).
40. Liu, A. et al. A molecular insight of Hes5-dependent inhibition of myelin gene expression: old partners and new players. *Embo J* **25**, 4833-42 (2006).
41. Poliakov, A., Cotrina, M. & Wilkinson, D. G. Diverse roles of eph receptors and ephrins in the regulation of cell migration and tissue assembly. *Dev Cell* **7**, 465-80 (2004).
42. Pasquale, E. B. Eph receptor signalling casts a wide net on cell behaviour. *Nat Rev Mol Cell Biol* **6**, 462-75 (2005).
43. Goldshmit, Y., McLenachan, S. & Turnley, A. Roles of Eph receptors and ephrins in the normal and damaged adult CNS. *Brain Res Rev* **52**, 327-45 (2006).
44. Lu, Q., Sun, E. E., Klein, R. S. & Flanagan, J. G. Ephrin-B reverse signaling is mediated by a novel PDZ-RGS protein and selectively inhibits G protein-coupled chemoattraction. *Cell* **105**, 69-79 (2001).
45. Schmucker, D. & Zipursky, S. L. Signaling downstream of Eph receptors and ephrin ligands. *Cell* **105**, 701-704 (2001).
46. Massague, J., Seoane, J. & Wotton, D. Smad transcription factors. *Genes Dev* **19**, 2783-810 (2005).
47. Hall, A. K. & Miller, R. H. Emerging roles for bone morphogenetic proteins in central nervous system glial biology. *J Neurosci Res* **76**, 1-8 (2004).

48. Sanderson, M. P., Dempsey, P. J. & Dunbar, A. J. Control of ErbB signaling through metalloprotease mediated ectodomain shedding of EGF-like factors. *Growth Factors* **24**, 121-136 (2007).
49. Binnerts, M. E. et al. R-Spondin1 regulates Wnt signaling by inhibiting internalization of LRP6. *Proc Natl Acad Sci U S A* **104**, 14700-5 (2007).
50. Court, F. A., Wrabetz, L. & Feltri, M. L. Basal lamina: Schwann cells wrap to the rhythm of space-time. *Curr Opin Neurobiol* 16, 501-7 (2006).
51. Szuchet, S. in *Neuroglia* (eds. Kettenmann, H. & Ransom, B.) 23-43 (Oxford University Press, New York, 1995).
52. Gregori, N., Proschel, C., Noble, M. & Mayer-Proschel, M. The tripotential glial-restricted precursor (GRP) cell and glial development in the spinal cord: generation of bipotential oligodendrocyte-type-2 astrocyte progenitor cells and dorsal-ventral differences in GRP cell function. *J Neurosci* **22**, 248-56 (2002).
53. Strathmann, F. G., Wang, X. & Mayer-Proschel, M. Identification of two novel glial-restricted cell populations in the embryonic telencephalon arising from unique origins. *BMC Dev Biol* **7**, 33 (2007).
54. Baracskay, K. L., Kidd, G. J., Miller, R. H. & Trapp, B. D. NG2-positive cells generate A2B5-positive oligodendrocyte precursor cells. *Glia* **55,** 1001-10 (2007).
55. Taniike, M. et al. Perineuronal oligodendrocytes protect against neuronal apoptosis through the production of lipocalin-type prostaglandin D synthase in a genetic demyelinating model. *J Neurosci* **22**, 4885-96 (2002).
56. Urade, Y. et al. Dominant expression of messenger RNA for prostaglandin-D synthase in leptomeninges, choroid plexus, and oligodendrocytes of the adult rat brain. *Proceedings of the National Academy of Sciences USA* **90**, 9070-9074 (1993).
57. Fujimori, K., Kadoyama, K. & Urade, Y. Protein kinase C activates human lipocalin-type prostaglandin D synthase gene expression through de-repression of Notch-HES signaling and enhancement of AP-2β function in brain-derived TE671 cells. *J Biol Chem* **280**, 18452-18461 (2005).
58. Yamazaki, Y. et al. Direct evidence for mutual interactions between perineuronal astrocytes and interneurons in the CA1 region of the rat hippocampus. *Neuroscience* **134**, 791-802 (2005).

59. Lin, S.-c. & Bergles, D. E. Synaptic signaling between GABAergic interneurons and oligodendrocyte precursor cells in the hippocampus. *Nat Neurosci* **7**, 24-32 (2004).
60. Ludwin, S. K. & Sternberger, N. H. An immunohistochemical study of myelin proteins during remyelination in the central nervous system. *Acta Neuropathologica* **63**, 240-248 (1984).
61. Aguirre, A., Dupree, J. L., Mangin, J. M. & Gallo, V. A functional role for EGFR signaling in myelination and remyelination. *Nat Neurosci* **10**, 990-1002 (2007).
62. Kanehisa, M. et al. From genomics to chemical genomics: new developments in KEGG. *Nucleic Acids Res* **34**, D354-7 (2006).

Supplementary Information: Full Methods and additional Figures are available on the online version of the paper at www.nature.com/nature

Acknowledgements

Most of this work was done in the Section of Developmental Neurogenetics (NINDS, NIH) where SS – a recipient of a NRSA award - was on sabbatical leave from The University of Chicago. The authors thank Drs. Robert Miller, Anthony Reder and Miriam Domowicz for reading the manuscript and Dr. Vittorio Gallo for the CNP/GFP transgenic mice. The authors gratefully acknowledge the assistance of Drs Abdel Elkahloun and Carolyn Smith of the NINDS Microarray and Imaging Facility, respectively. Supported by intramural NINDS funds and in part by a Pilot Project (SS) from the National Multiple Sclerosis Society.

Author Information

The raw data will be deposited in the Gene Expression Omnibus accessible at http://www.ncbi.nlm.nih.gov/geo/

The authors have no conflicts of interests

Correspondence and request for materials should be addressed to SS (szuchet@neurology.bsd.uchicago.edu) or LDH (hudsonl1@od.nih.gov)

Figure Legends

Figure 1. The polyclonal antibody OTMP recognizes perineuronal oligodendrocytes in cortical gray matter but does not stain neurons or astrocytes. Rat (A-C) and human (D) brain sections were labelled for OTMP (red-A,B; green-C), NeuN (green-A,B; red-C), and DAPI (blue) for confocal (A-C) or epifluorescence (D) microscopy. Notice that OLGs actually indent the neuronal soma (arrows in A and D) and their processes envelop the neuron (arrowheads in B). Arrowhead in D points to a nucleus abutting a neuron that is not stained by OTMP (astrocyte or microglial cell?). There is no overlap between OTMP and NeuN, i.e., OTMP does not stain neurons. E-G presents sections of a rat corpus callosum double stained with GFAP (E, green) and OTMP (F, red). Merge in G shows no co-localization with GFAP. Scale bar = 10 μm

Figure 2. OTMP$^+$ perineuronal cells are of OLG lineage but do not synthesize myelin proteins. Arrows in A-C point to a perineuronal cell in the cortex of a 7-day-old CNP/EGFP transgenic mouse double stained with anti-GFP (A, green) and OTMP (B, red). The overlap of the two (C) demonstrates that pN-OLGs are OLG precursor's progeny. Arrows in D-F direct to a pN-OLG from a P14 rat cortex double labelled for OTMP (D, green) and MBP (E, red). Note the absence of MBP (E) in the perineuronal cell and the strong presence of MBP in the myelinated fibers (arrowheads in E and F). Panel F (merge) confirms that pN-OLGs do not synthesize MBP.

Figure 3. $A_2B_5^+$/$OTMP^+$cells are scattered throughout the developing brain. Panels **A** (P7) and **B** (P14) illustrate a representative fluorescence-activated cell sorting experiment, which addresses the distribution of acutely isolated OLG progenitors double labelled with A_2B_5 and OTMP. Each graph is divided into upper left (UL), upper right (UR), lower left (LL), and lower right (LR) quadrants, depicting $OTMP^-/A_2B_5^+$, $OTMP^+/A_2B_5^+$, $OTMP^-/A_2B_5^-$ and $OTMP^+/A_2B_5^-$ cell phenotypes, respectively. The percentage of cells found in the individual quadrants is indicated as the percent gated. There is heterogeneity in the intensity of staining within both the single and the double labelled cells. Quantitatively there are no appreciable changes in cell dispersion between P7 and P14.

Figure 4. The $A_2B_5^+$/$OTMP^+$ cell depicts a unique oligodendrocyte lineage phenotype. We used Affymetrix microarray technology to identify gene expression patterns for P7 cells recognized by four molecular markers $A_2B_5^+$, $A_2B_5^+/OTMP^+$, O_4^+ and $OTMP^+$. The Principal Component Analysis (A) disclosed a sharp demarcation among the different populations. Noteworthy, is the observation that the OTMP antibody identifies a subpopulation of $A_2B_5^+$ precursors with a different phenotype. B and C illustrate two general gene expression patterns of the $A_2B_5^+/OTMP^+$ phenotype compared to both $A_2B_5^+$ and O_4^+ cells. In D the expression patterns of transcription factors demonstrated to be critical for the development of OLGs are compared for the three subpopulations.

Figure 5. Signalling pathways and molecules important to the $A_2B_5^+$/$OTMP^+$ phenotype. We have used the Ingenuity software to analyze $A_2B_5^+/OTMP^+$gene expression data either as interacting networks or as canonical pathways. Red denotes upregulation and green downregulation of transcripts in the $A_2B_5^+/OTMP^+$ relative to $A_2B_5^+$ precursor (F) or the O_4^+ committed OLG (A-E). Edge types: solid line = direct action; broken line = indirect action;

arrow from A to B = act on; line joining A to B = binding only; line ending in vertical dash=inhibits. **A.** This network illustrates upregulation of transcripts for *pdgfr-α* (arrowhead), *pdgfr-β* (arrowhead), and cytokine *pdgf-c* (asterisk). Their interaction should eventuate in the expression of the heterodimer PDGFR-αβ on the surface of the $A_2B_5^+$/OTMP$^+$ cell, silencing its response to PDGF-AA – a ligand for the myelinating OLG, and thereby, segregating the two cell types. Note also the down*regulation* of *pdgf-a* (double arrow). That sonic hedgehog (Shh) has a role in the increased (7.2-fold) transcription of *pdgfr- α* can be surmised from Fig. S4. The growth factor receptor (double asterisks) implicated in the regulation of the other components remains to be elucidated. A cross-talk with Notch signalling (>4-fold increase in Hey1; large arrow) is hinted by its apparent involvement in the increased expression (3.3-fold) of phospholipase C-γ (small arrow). **B.** $A_2B_5^+$/OTMP$^+$ transcripts pertaining to Wnt signalling are shown in an interacting network. Asterisks mark the receptors Fzd, co-receptor LRP6, and the protein DVL1 (dishevilled); they are all upregulated. Notice that NrCAM (arrowhead) appears as a cell specific target of Wnt signalling. **C.** This network illustrates three aspects of Notch signalling (asterisk):1**.** (large arrow) upregulation of ASCL1/Mash1; 2**.** (arrowhead) increased expression (>13-fold) of Hes5; 3. (small arrow) enhanced transcription of lipocalin-prostaglandin D2 synthase (L-PGDS). Inset shows an OTMP$^+$/L-PGDS$^+$ pN-OLG demonstrating that the L-PGDS protein is expressed. **D.** $A_2B_5^+$/OTMP$^+$ transcripts were analyzed using the canonical pathway for the Eph/ephrin tyrosine kinases. Small arrows point to the upregulated EphA receptors. Arrowhead signals the ephrin B receptor. Asterisks denote the G-coupled CXCR4 receptor and its ligand SDF-1, which together with ephrin B may play a role in cell migration.

Figure 6. The ECM matrix of $A_2B_5^+$/OTMP$^+$ cells (see Fig. 5 for a description of the method of analysis and the meaning of symbols). **A**. Asterisks point to the different collagens that are

secreted by the $A_2B_5^+$/$OTMP^+$ cells. Small and large arrow, respectively, indicate reelin and nidogen. Note that SMAD7 (double arrows) may regulate the secretion of some of the collagens. **B.** Asterisks mark secreted BMPs; arrowheads point to their receptors; arrow indicates the receptor endoglin. Note the role of SMAD7 (double arrows). **C.** This network illustrates the role of the kinase ERB-b2 (double arrow) in the shaping of the ECM of the $A_2B_5^+$/$OTMP^+$cells. Asterisks point to MMPs; arrowhead signals their inhibitor, TMP; small arrow indicates the chondroitin sulphate proteoglycan, versican. **D. T**his network demonstrates the cross-talk between the ECM and the cell (see text).

Supplementary Information

Methods

Immune-purified polyclonal antibody, OTMP. A 20 amino acid peptide of sheep OTMP (residues 254-273) was synthesized, coupled to a carrier and injected into two rabbits (Biosource, Inc. Camarillo, CA). Following testing by ELISA and immunohistochemistry, the most active batch of serum was purified on a peptide-affinity column.

Immunohistochemistry of rodent and human brain. Free-floating sections were blocked with 3% normal goat serum (NGS) in PBS containing 0.1% Triton X-100 for 1½ h at room temperature. Primary antibodies (Abs) were applied overnight at 4°C. Affinity purified polyclonal rabbit anti-OTMP (1:200) was used in combination with Abs for the identification of: 1) neurons (anti-NeuN, 1:500; Chemicon, Temacula, CA); 2) oligodendrocytes-CC1/Ab7/APC, 1:350, Oncogene Research Products, Boston, MA), anti-CNPase (1:500, Sternberger Monoclonals, Lutherville, MD), anti-MBP, (1:1000, Covance); 3) microglial cells, (anti-Iba1, Wako Chemicals, Richmond, VA); 4) astrocytes (anti-GFAP, 1:1,000, Sigma, St. Louis, MO). After three washes with PBS, sections were incubated for 1½ h with anti-rabbit IgG labeled with

Alexa Fluor 594 (1:800) and anti-mouse IgG labeled with Alexa Fluor 488 (1:800) (Molecular Probes, Eugene, OR). The sections were washed with PBS, mounted onto slides and covered using Vectashield with DAPI. Two types of controls were included: 1) primary Ab was replaced by pre-immune serum; 2) primary Ab was omitted. Images were captured with an Olympus fluorescent microscope fitted with a Cool Snap digital camera (Photometrics, Tucson, AZ). Confocal images were taken with a Zeiss LSM 410 laser scanner microscope with a 25X Plan Neofluor Objective and a 2X or 3X Zoom. The excitation wavelengths used were: 413 nm for DAPI, 488 nm for green and 543 nm for red fluorescence.

Human tissue. The dissected tissue blocks were fixed in 4% paraformaldehyde for 2 weeks. Free-floating brain sections (15 μm) obtained with a vibratome (Leica WT1000S) were treated with 10% NGS for 1h to reduce non-specific binding followed by incubation for 48 hr at 10˚C with primary Abs diluted in PBS containing 1% NGS: OTMP (1:300), NeuN (1:600), CC1 (1:400). Immunoreactivity was visualized with species-specific secondary Abs (1:300) conjugated to either Alexa Fluor 488 or Alexa Fluor 594. The free-floating sections were mounted onto glass slides and coverslipped with Vectashield mounting medium containing DAPI. Signal was visualized using an inverted epifluorescence microscope (Olympus BX51). Images were acquired using a cooled digital camera controlled by Analysis Lab Digital imaging software. The contrast and brightness of the digitally acquired images were adjusted with Adobe Photoshop 5.5.

Cell preparation and sorting. We followed the protocol described by Nielsen, *et al.*[16] Briefly, whole brains were dissected from postnatal day 7 Sprague-Dawley rats, and the cerebellum and meninges were removed in 4˚C Hank's Balanced Salt Solution. Brains were dissociated using gentle trituration, followed by a 10 min papain and a 10 min DNase I digestion. A 15%-40%

Percoll gradient was used to purify cells away from myelin debri. The OTMP Ab was used in combination with the IgM mAb A_2B_5 (Eisenbarth *et al.,* 1979), and the IgM mAb O_4 (Sommer and Schachner, 1981; Gard and Pfeiffer, 1990). The latter two Abs were produced and purified from hybridoma cultures grown in house. The O_4 labeling was detected using goat anti-mouse IgM conjugated with Alexa Fluor 488. Normal mouse IgM was used to block excess IgM binding sites before detection of A_2B_5. A_2B_5 was custom-conjugated with biotin using a standard biotinylation kit (Pierce, Rockford, IL), according to manufacturer's specifications, and visualized with streptavidin conjugated with phycoerythrin (PE) and Texas red (TxR) tandem dye (Caltag). OTMP was detected with anti-rabbit IgG conjugated to PE. Labeled cell suspensions were physically sorted directly into collection tubes containing RNAlater (Ambion, Austin, TX) using a FACSVantageSE flow cytometer (Becton Dickinson, Franklin Lakes, NJ). FITC, PE, PE-TxR, and PE-Cy5 were excited by an argon laser (model 2016, Spectra Physics, Mountain View, CA) and the resulting emission was collected with bandpass filters at 530±30nm, 575±25nm, 615±10nm, and 670±20nm. Cell Quest Acquisition and analysis software was used to quantify fluorescence signal intensities and cell numbers in each cell population.

Microarray. 10 μg of biotin-labeled and fragmented cRNA was hybridized to Affymetrix Rat expression 230 microarrays (Affymetrix, Santa Clara, CA). The microarrays were hybridized, washed and scanned according to Affymetrix standard protocols. Genespring analysis software was used for RMA pre-processing of the raw CEL files and for normalization. The data were normalized using a per chip normalization (normalized to the 50^{th} percentile) and per gene normalization (normalized to the median). A 2-fold difference in normalized expression value was used to identify differentially regulated transcripts. In addition, a Welch t-test was performed without an assumption of equal variances. The Benjamini and Hochberg multiple

testing correction was used with a false discovery rate of 0.05. The two-fold cutoff and the statistical test were used to obtain the differentially regulated gene lists.

Immunocytochemistry of cutured live rat oligodendrocytes. $A_2B_5^+$ oligodendrocyte progenitors (OLP) FACS purified were maintained as such by supplementing the medium with growth factors by way of a conditioned medium from a neuroblastoma (B104) cell line. The cells switch to an OLG phenotype (differentiate) following removal of the conditioned medium. The two phenotypes have characteristic morphologies and express different surface markers. The progenitor is mostly bipolar and is marked by the mAb A_2B_5, whereas the young OLG is mainly multipolar and is stained by the mAb O_4.

We double stained live cells with either A_2B_5/OTMP or O_4/OTMP. For this we used the regular medium containing either mAb A_2B_5 or mAbO_4 (1:500) and polyclonal anti-OTMP (1:100) and cells were placed back in the incubator for 30 min. Medium was then removed and cultures were washed twice with PBS (Ca^2+Mg^2), fixed with 4% paraformaldehyde in PBS (Ca^2 + Mg^2) for 10 min, and washed with PBS 3 times for 10 min each. The secondary Abs, goat α-mouse IgM (A_2B_5 or O_4) Alexa-Fluor 488 (green)/goat α-rabbit IgG (OTMP) Alexa-Fluor 594 (red) at 1:700 in PBS containing 3% normal goat serum (NGS; Gibco, Long Island. NY) were applied for 2hr before slides were washed once for 15 min and 4 times for 5 min, then mounted with Vectashield containing diamidino 2-phenylindol-HCl (DAPI) (Vector Laboratory, Burlingham, CA).

Supplementary Figure L**egends**

Figure S1. The antibody OTMP stains live rat oligodendrocyte progenitors. Staining of live rat OLGs with A_2B_5 (green) or O_4 (green) and OTMP (red). A-C: progenitors, notice co-localization A_2B_5 and OTMP (B). D-F: differentiated OLGs, no co-localization of O4 and OTMP in the fully differentiated cell (C).

Figure S2. Developmental distribution of $A_2B_5^+$/$OTMP^+$ cells in different brain compartments. CNS tissue was fractionated into spinal cord, brain stem, basal ganglia, corpus callosum, and cortex at P0, P7 and P14. Acutely isolated cells were double labelled with mAb A_2B_5 and OTMP and fractionated by fluorescence-activated cell sorting. Each graph is divided into upper left (UL), upper right (UR), lower left (LL), and lower right (LR) quadrants, depicting $OTMP^-/A_2B_5^+$, $OTMP^+/A_2B_5^+$, $OTMP^-/A_2B_5^-$ and $OTMP^+/A_2B_5^-$ cell phenotypes, respectively. The percentage of cells found in the individual quadrants is indicated as the percent gated. **A.** P0; **B.** P7; **C.** P14. (See text for results.)

Figure S3. Expression of *dlx1 and pax6* in $A_2B_5^+$/$OTMP^+$ cells. Arrowheads point to the upregulation of *dlx1 and pax6;* asterisks signal the downregulation of *sox2* and *nkx2.2.* Note that these events appear to be interrelated.

Figure S4. Participation of sonic hedhehog (Shh) in the fate of $A_2B_5^+$/$OTMP^+$ cells. The network shows the upregulation of Shh receptors, Patched and Smoothened (arrowheads) and the transcription regulators Gli1-3 (asterisk). There is an indication that Shh plays a role in the increased expression of PDGFR-α.

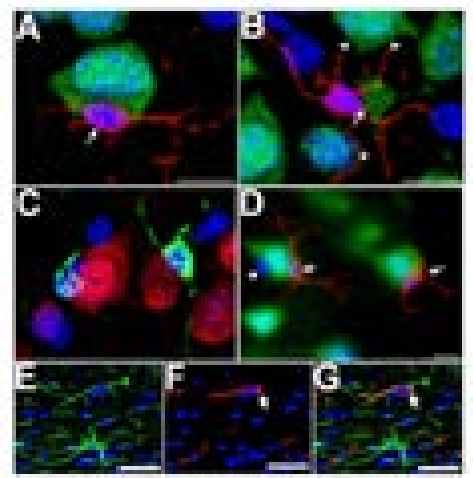
A
B
C
D
E
F
G

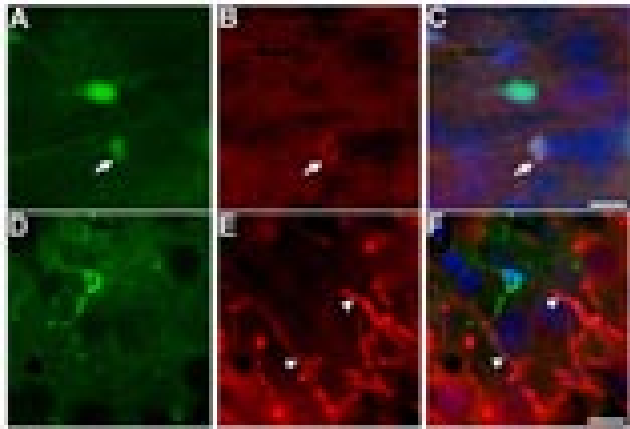
A
B
C
D
E
F

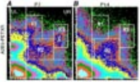

Quadrant	% Gated
UL=A205+/OTMP-	19.2
UR=A205+/OTMP+	11.2
LL=A205-/OTMP-	48.5
LR=A205-/OTMP+	22.1

Quadrant	% Gated
UL=A205+/OTMP-	11.3
UR=A205+/OTMP+	9.1
LL=A205-/OTMP-	55.5
LR=A205-/OTMP+	23.5

Region	% Gated	OTMP Mean	A205 Mean
R1	2.1	27.6	600.3
R2	5.5	183.6	92.1
R3	1.8	1490.8	195.2

Region	% Gated	OTMP Mean	A205 Mean
R1	0.5	61.1	446.5
R2	8.5	133.5	46.5
R3	0.8	1384.8	232.2

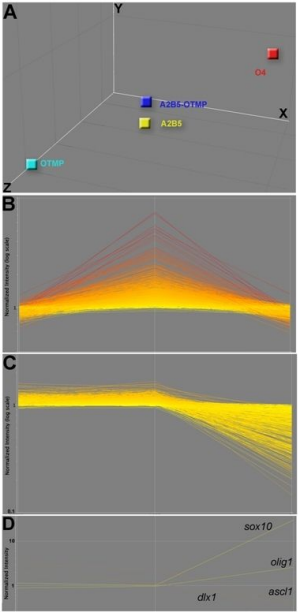
A
Y
O4
A2B5-OTMP
X
A2B5
OTMP
Z
B
Normalized Intensity Per Cell
C
Normalized Intensity Per Cell
D
Normalized Intensity Per Cell
sox10
olig1
ascl1
dlx1
A2B5
A2OT
O4


A
B
C
D

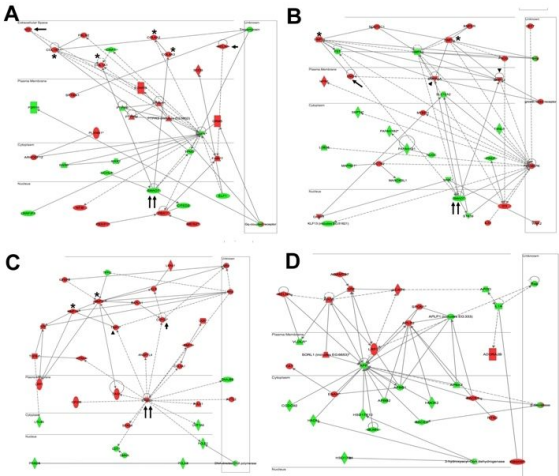
A
B
C
D

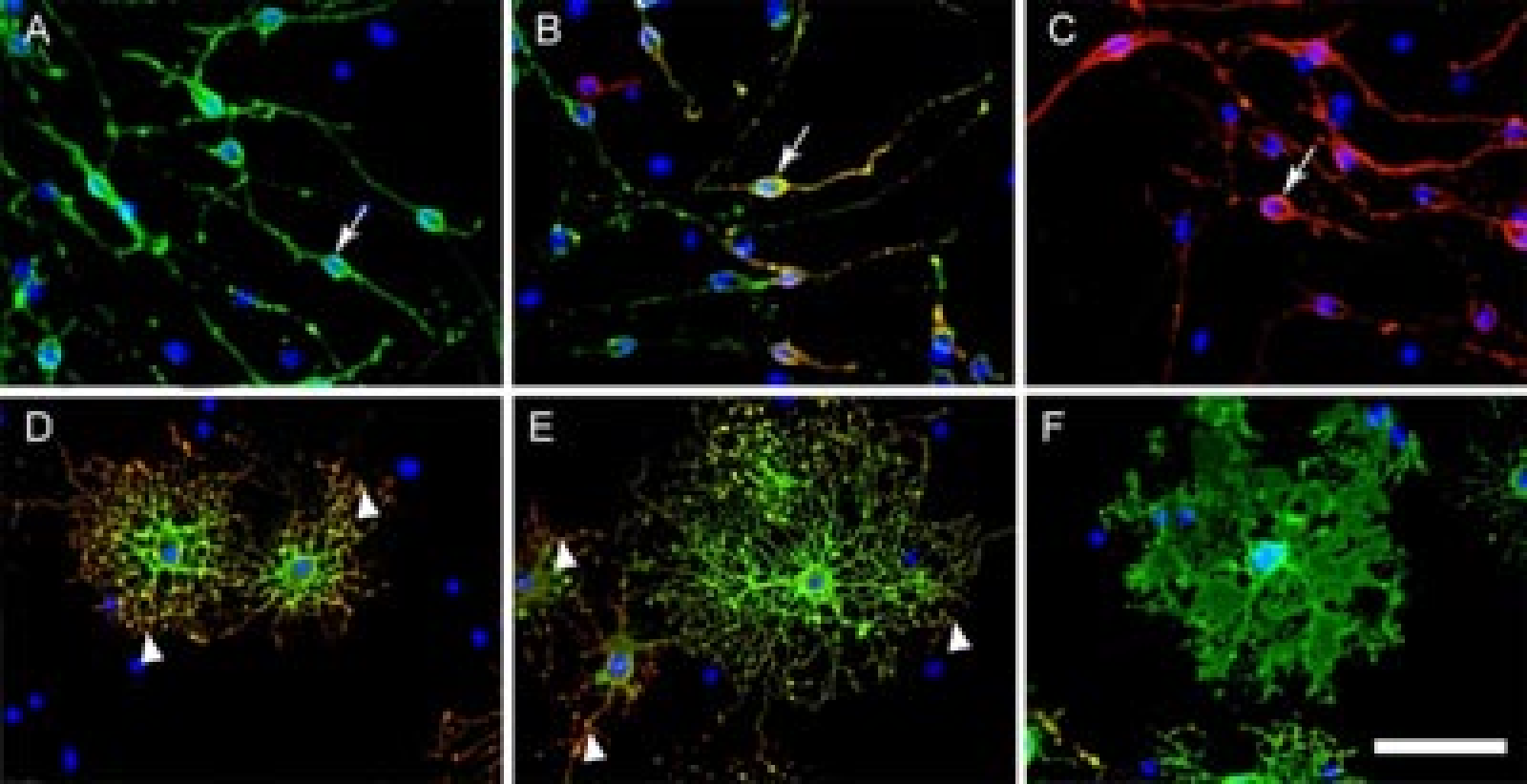
A
B
C
D
E
F

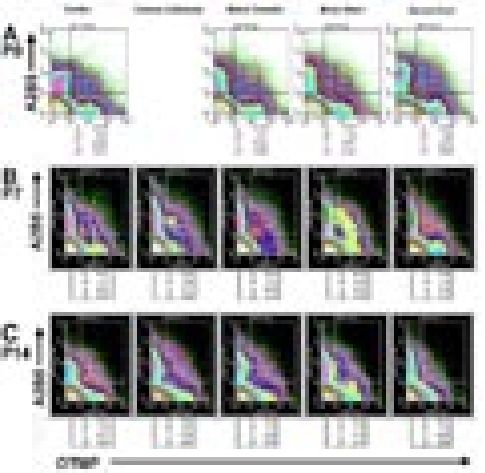
A
B
C
CTRP

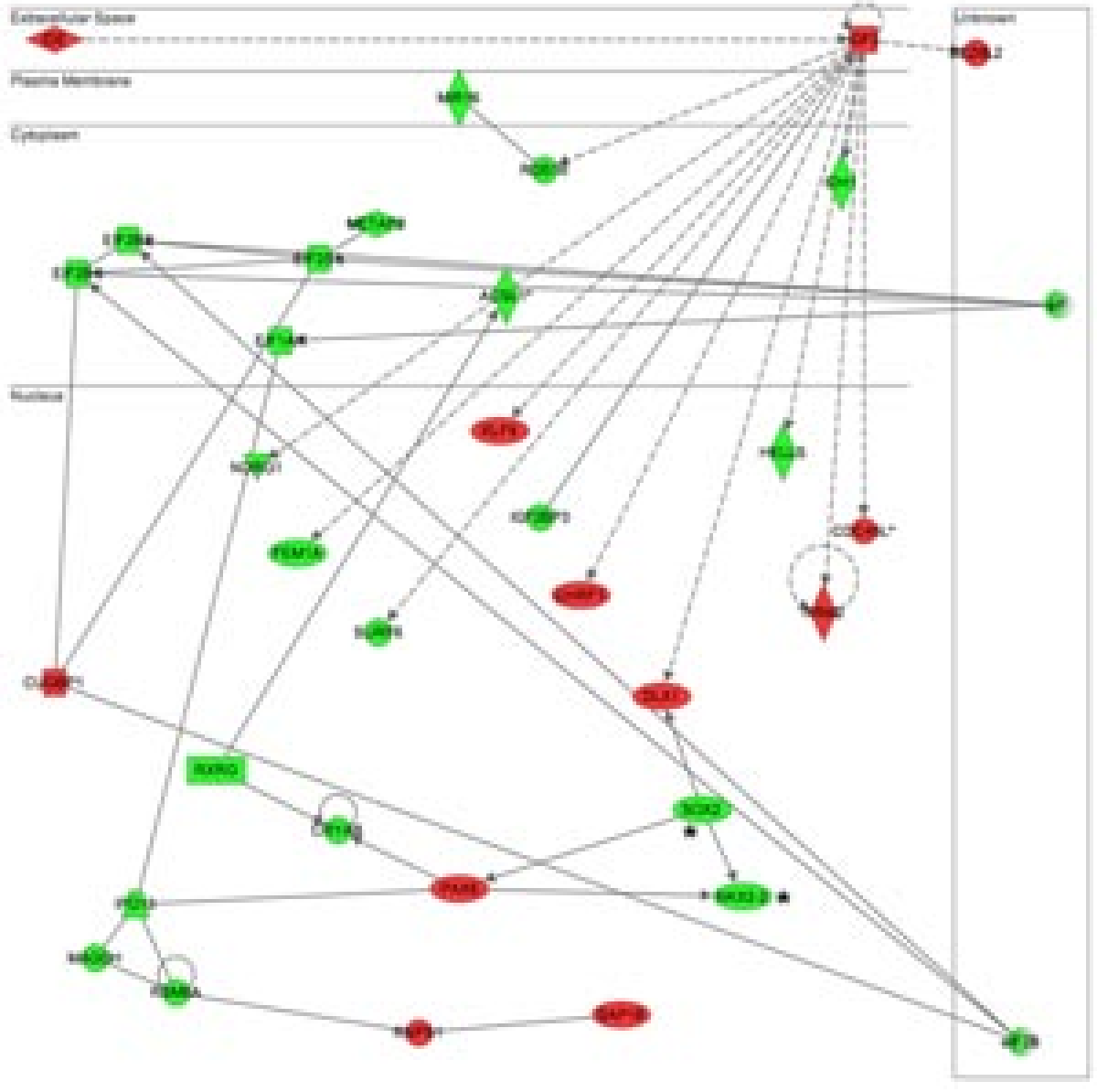
Extracellular Space
Plasma Membrane
Cytoplasm
Nucleus
Unknown